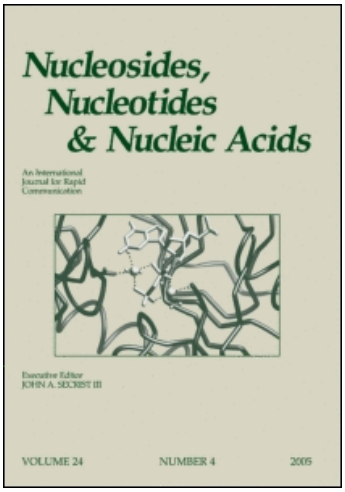

Nucleosides, Nucleotides and Nucleic Acids
Publication details, including instructions for authors and subscription information:
http://www.informaworld.com/smpp/title~content=t713597286

Structure of the Trinucleotide D-acp³U-A with Coordinated Mg^{2} Demonstrates that Modified Nucleosides Contribute to Regional Conformations of RNA

John W. Stuart[a]; Mufeed M. Basti[a]; Wanda S. Smith[a]; Brian Forrest[a]; Richard Guenther[a]; Hanna Sierzputowska-Gracz[a]; Barbara Nawrot[b]; Andrzej Malkiewicz[b]; Paul F. Agris[ab]
[a] Department of Biochemistry, North Carolina State University, Raleigh, North Carolina [b] Institute of Organic Chemistry, Technical University, Lodz, Poland

To cite this Article Stuart, John W. , Basti, Mufeed M. , Smith, Wanda S. , Forrest, Brian , Guenther, Richard , Sierzputowska-Gracz, Hanna , Nawrot, Barbara , Malkiewicz, Andrzej and Agris, Paul F.(1996) 'Structure of the Trinucleotide D-acp³U-A with Coordinated Mg^{2} Demonstrates that Modified Nucleosides Contribute to Regional Conformations of RNA', Nucleosides, Nucleotides and Nucleic Acids, 15: 5, 1009 — 1028
To link to this Article: DOI: 10.1080/07328319608002031
URL: http://dx.doi.org/10.1080/07328319608002031

NUCLEOSIDES & NUCLEOTIDES, 15(5), 1009-1028 (1996)

STRUCTURE OF THE TRINUCLEOTIDE D-acp^{3}U-A WITH COORDINATED Mg^{2+} DEMONSTRATES THAT MODIFIED NUCLEOSIDES CONTRIBUTE TO REGIONAL CONFORMATIONS OF RNA

John W. Stuart[+], Mufeed M. Basti[+], Wanda. S. Smith[+#], Brian Forrest[+#], Richard Guenther[+], Hanna Sierzputowska-Gracz[+], Barbara Nawrot[•#], Andrzej Malkiewicz[•] and Paul F. Agris[+*]

[+]Department of Biochemistry, North Carolina State University, Raleigh, North Carolina 27695-07622

[•]Institute of Organic Chemistry, Technical University, Lodz, Poland

Abstract: In tRNA crystal structures, the only nonaromatic ribonucleoside, dihydrouridine (D) and 3'-adjacent nucleotides adopt the infrequent 2'-endo conformation. Analysis of D, DUA and UUA by circular dichroism (CD) and NMR confirmed that D produces the 2'-endo conformation of the trimer and is responsible for the same in tRNA. The nucleoside, 3-[3-(S)-amino-3-carboxypropyl]uridine (acp^{3}U) occurs in the tRNA sequence D-acp^{3}U-A. CD spectra indicated that D-acp^{3}U-A and U-acp^{3}U-A bind Mg^{2+}, whereas acp^{3}U, D-acp^{3}U, DUA and UUA do not. Ion dependent changes in chemical shifts and paramagnetic broadening of ^{1}H signals indicated that Mg^{2+} coordination involved the acp$_3$U side chain and the ribose of A. The Mg^{2+}-bound structure was modeled with simulated annealing, molecular mechanics and NMR restraints. Acp^{3}U contributed to local charge density that facilitated Mg^{2+} coordination.

Introduction

The chemistries of the four standard bases are inadequate for all the functional activities of tRNA. Posttranscriptionally modified bases make important contributions to the RNA's native structure and function.[1] For instance, modifications constrain

* To whom inquiries should be addressed at the Department of Biochemistry, 128 Polk Hall, Box 7622 North Carolina State University, Raleigh, NC 27695-7622

Present addresses: W.W.S., NMR Facility University of California, Davis, CA; B.F., School of Medicine, University of North Carolina, Chapel Hill, NC; B.N., Lab for Biochemistry, University of Bayreuth, Bayreuth, Germany.

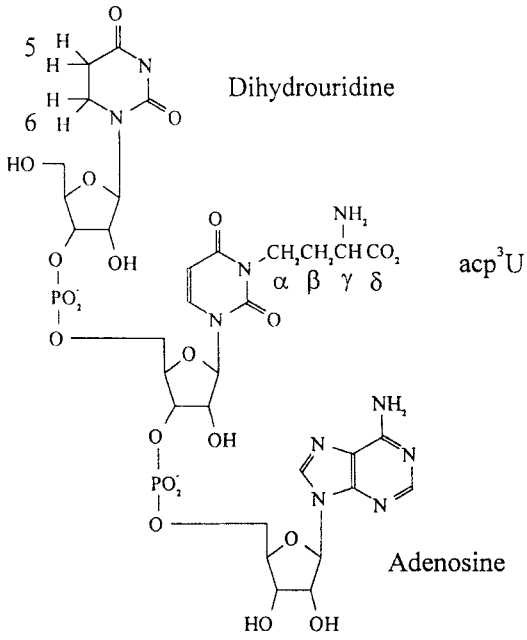

FIG. 1: Chemical structure of D-acp^{3}U-A showing the modified uridines: D and acp^{3}U.

ribose conformation and confer metal binding capability. Some of the most interesting and varied modified nucleosides are the uridines. One of the modified uridines, dihydrouridine (D[1]), is the only nonaromatic nucleoside.[2] Loss of π-π interactions prevents D from contributing to base stacking. The saturated C_5-C_6 bond length is increased to about 1.50 Å and the added volume due to the additional protons on C_6 influences the sugar pucker of D.[3] In contrast to all other unmodified and modified ribonucleosides, D strongly prefers the 2'-endo conformation altering the δ torsion angle and exposing the base.[4] D is found in 77% of native tRNA sequences at a number of positions in the D-loop and at position 47 in the extra loop (Figure 1).[5] In

[1]Abbreviations used: Dihydrouridine, D; 3-[3-(S)-amino-3-carboxy-propyl]-uridine, acp^{3}U; 3-[3-(S)-amino-3-carboxy-propyl], acp^3 side chain; circular dichroism, CD; nuclear Overhauser effect, NOE; two-dimensional NOE spectroscopy, NOESY; two dimensional rotating frame nuclear Overhauser effect spectroscopy, ROESY; simulated annealing, SA; references to minimization denote energy minimization.

tRNA crystal structures the 2'-endo conformation is observed in the 3'-adjacent nucleosides.[6] Though D is thought to be responsible for inducing 2'-endo conformation in downstream nucleotides, experimental evidence is lacking.

Another modified uridine, the nucleoside 3-[3-(S)-amino-3-carboxypropyl]uridine (acp^{3}U), has chemical properties that contrast with those of D. Under physiological conditions the primary amine is unprotonated and the carboxylic acid is deprotonated.[7,8] While acp^{3}U occurs in 8% of known tRNA sequences it may be representative of nucleosides with amino acid side chains such as N-6-(threonylcarbamoyl)-adenosine (t^{6}A) and N-6-(glycylcarbamoyl)adenosine (g^{6}A). Acp^{3}U occurs at position 20 and 47 in regions strongly involved with tertiary structure and metal binding. The role of acp^{3}U is currently unknown.

The sequence D-acp^{3}U-A occurs in the D-loop of tRNA from eukaryotic species ranging from *Lupinus luteus* to human.[5] In tRNAs of *E. coli*, acp^{3}U occurs in the extra loop with 7-methylguanosine (m^{7}G) in the sequence m^{7}G-acp^{3}U-C. Tandem modified nucleotides occur frequently in tRNA molecules. Elucidating the effect that D and acp^{3}U have on one another and on unmodified adjacent nucleosides can help us understand their purpose in mature tRNA molecules. Here, we report that D promotes 2'-endo sugar pucker in its 3' neighbors. We also show that acp^{3}U requires an adjacent nucleoside to induce a Mg^{2+} binding site. Further when the two modified nucleosides occur in tandem, the individual contributions are enhanced.

Results

Modifications change oligomer conformation. To determine the conformations of the nucleosides within each oligomer, coupling constants were measured from homonuclear, J_{HH} coupled NMR spectra and the conformational parameters calculated (Table I). The mononucleoside D had an 88% fractional population in the 2'-endo conformation. The conformation of D was further restricted to 95% 2'-endo conformation in the dimer and trimers. Acp^{3}U was 40% 2'-endo as a monomer, and 47% 2'-endo in the dimer D-acp^{3}U. Significantly when D is in the first position, acp^{3}U and U in the trimers were 63 and 72% 2'-endo, respectively.

Mg^{2+} alters oligonucleotide conformation. The presence of a modified nucleoside in an oligomer has been shown to cause a change in conformation upon the addition

Table I. Conformational Parameters and Changes Produced by Mg^{2+}[a]

	D	acp^{3}U	D-----acp^{3}U		D--------acp^{3}U------A			D--------U--------A			U----acp^{3}U-----A			U------U----A		
%N	12	60	5	53	3(~*0*)	37*(32)*	37	4	28	35	43	35	38	48	54	55
%γ^+	54	66	59	83	58	92	79	59	69	76	77	87	77	73	70	81
%ϵ^t	--	--	<23	--	41	64	--	22	67	--	22	84	--	84	80	--
%β^t	--	--	--	80	--	83	83	--	60	66	--	55	55	--	85	85
χ	a>s	a~s	a	a>s	a	a>s	a≫s	a>s	a>s	a>s	a>s	a>s	a>s	a>s	a>s	a>s

[a]New parameter after addition of Mg^{2+} displayed in *italics* right of original.

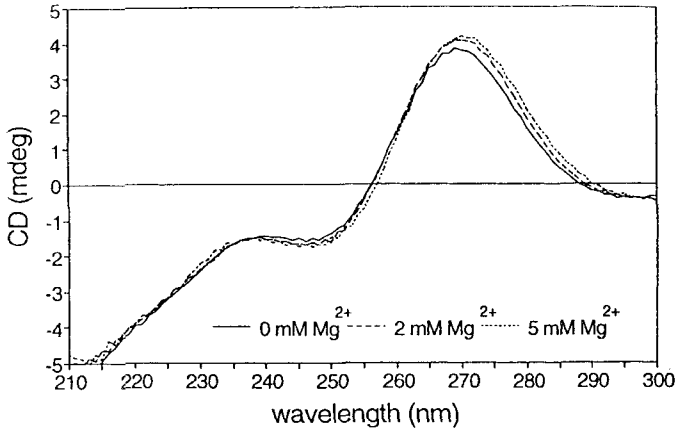

FIG 2: CD spectra of D-acp^{3}U-A; Mg^{2+} titration. D-acp^{3}U-A spectra were collected (10°C) with increasing [Mg^{2+}]: 0 to 5 mM Mg^{2+}. Spectra of the mononucleosides D, acp^{3}U and A, alone and together in equal molar proportions, were not effected by [Mg^{2+}]. Individual spectra could not be summed to obtain the spectrum of the trimer.

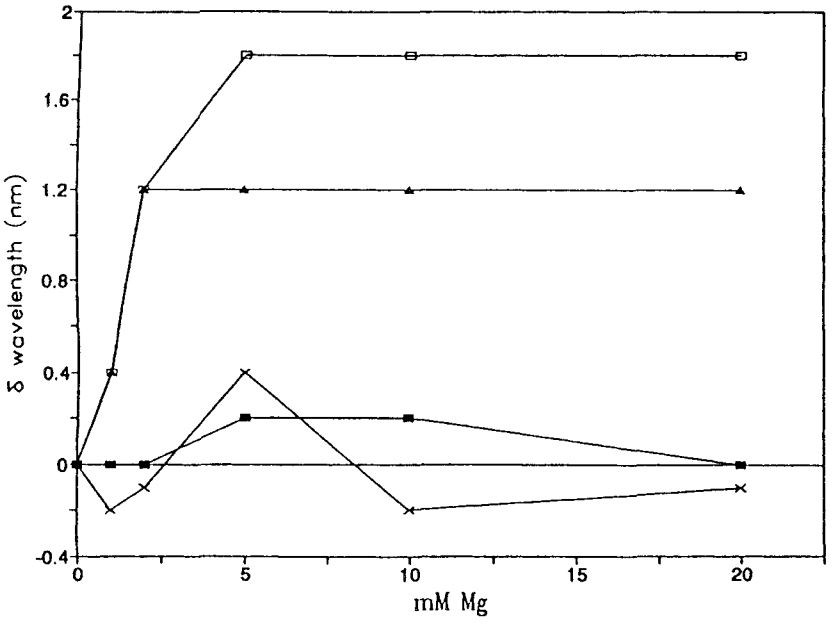

FIG 3: Changes in CD λ_{max} of D-acp^{3}U-A (□), DUA (X), U-acp^{3}U-A (▲) and UUA (■) as a function of [Mg^{2+}]: 0, 2, 5, 10 and 20 mM. Data for DUA (X) varied more than that of the other oligomers; D, with little absorbance, reduced the signal/noise more than that of D-acp^{3}U-A. No change observed in D-acp^{3}U.

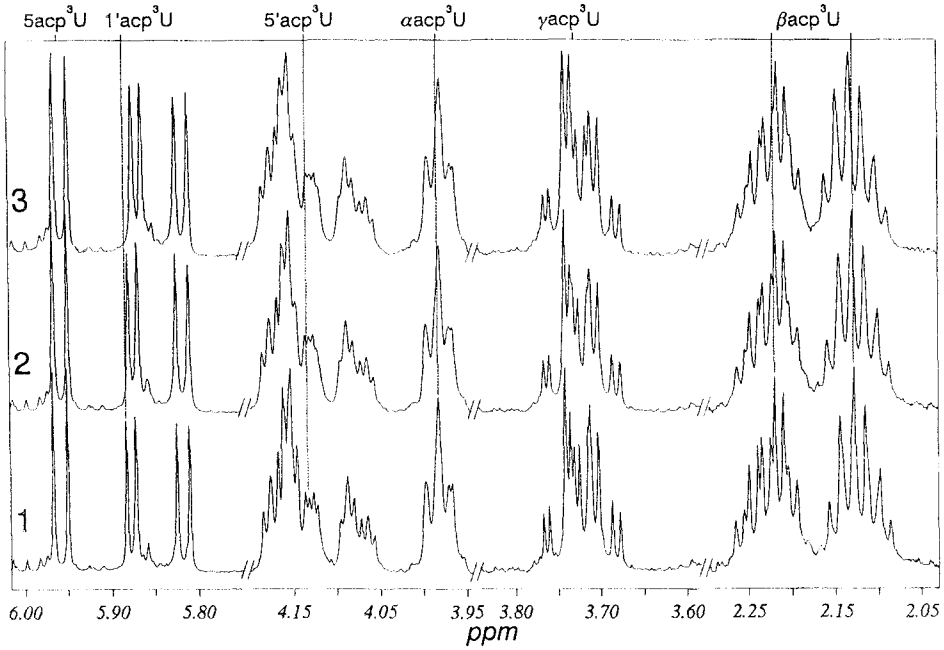

FIG 4: One-dimensional proton spectra of 1.5 mM D-acp^{3}U-A in phosphate buffered D_2O where traces 1–3 denote 0, 5 and 15 mM Mg^{2+}, respectively. Protons peaks that have shifted are indicated with labeled on the top and vertical lines.

of Mg^{2+}.[1] To monitor the affect of magnesium on the oligonucleotides, CD spectra were collected during titrations with Mg^{2+} from 0 to 20 mM. With the addition of Mg^{2+}, all of the trimers exhibited an increase in spectral amplitude at λ_{max} (Figure 2). However, trimers that contained acp^{3}U, D-acp^{3}U-A and U-acp^{3}U-A, in addition, displayed a red shift in λ_{max} (Figure 3). The λ_{max} for U-acp^{3}U-A did not change above 2 mM Mg^{2+}, whereas the λ_{max} for D-acp^{3}U-A continued to increase up to 5 mM Mg^{2+}. The same sensitivity to Mg^{2+} was observed in the CD spectra of the trimers at a 15 fold increase in trimer concentration indicating that this result was not due to a Mg^{2+} induced association of the trimers. With increasing Mg^{2+} concentrations, the CD spectra of the mononucleosides and the dimer D-acp^{3}U were neither changed in λ_{max} nor in the magnitude of ellipticity. Thus, the Mg^{2+}-dependent change in spectra required the trinucleotide structure.

To aid in determining the conformation of D-acp^{3}U-A in the presence of Mg^{2+}, ^{1}H and ^{13}C NMR spectra were acquired while titrating from 0 to 20 mM Mg^{2+} (Figure

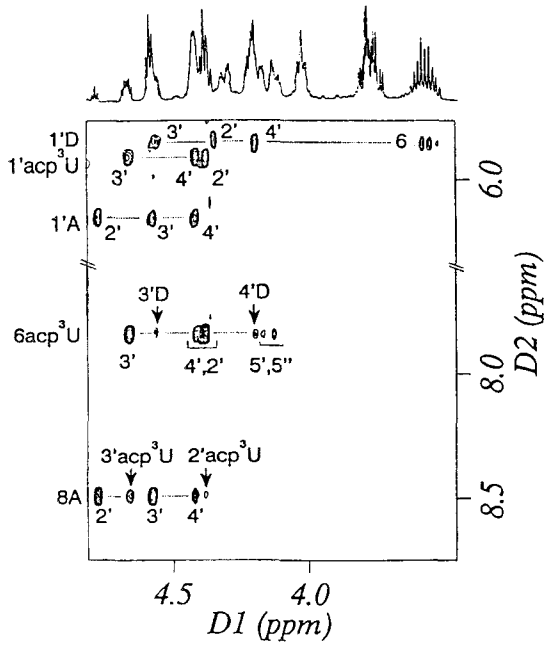

FIG 5: Two-dimensional ROESY spectrum (300-ms mixing time) of D-acp^{3}U-A in D_2O at 15°C. The regions of the spectrum for 1' to ribose NOE crosspeaks (upper section of figure) and aromatic to ribose crosspeaks (lower section) are shown. Intraresidue crosspeaks are denoted with horizontal dotted lines and interresidue crosspeaks are highlighted with arrows.

4). The presence of only one resonance per proton and the narrowness of the linewidth of the inter-residue ROESY crosspeaks was indicative of the trimer having either a single conformation or a small number of conformations in fast exchange. The most significant changes in ^{1}H chemical shifts with the addition of Mg^{2+} (Δ 2.5-5.0 Hz, absolute value) were recorded for the α, β, γ, 5, 6, 1' and 5' protons of acp^{3}U (Figure 4). The ^{13}C chemical shifts most significantly effected by Mg^{2+} (Δ 0.3-1.0 ppm) were the α, β, γ, 5 and 1' carbons of acp^{3}U and the 1' carbon of D (data not shown). The line width of these protons did not change and were on the same order as the unaffected proton signals of the riboses. This indicates that both before and after the addition of Mg^{2+}, we were observing stable conformers of acp^{3}U. ^{1}H and ^{13}C chemical shifts of A were not effected by addition of Mg^{2+} to D-acp^{3}U-A; no ^{31}P chemical shift change was observed.

Modeling of D-acp^{3}U-A. Distance restraints necessary to build a solution structure model were obtained from analysis of ROESY spectra in which all signals were assigned. Figure 5 shows a typical portion of the 300 ms ROESY spectrum with some of the assignments used in determining distance restraint data. We obtained 35 intra-residue and 10 inter-residue restraints (Table II). Since acp^{3}U was the center nucleotide and had a long side chain, it took part in 60 percent of the distance restraints and all of the inter-residue restraints. This was beneficial in defining the position of the acp side chain. From coupling constant data, dihedral restraints were calculated using the Karplus relationship. With an average of 15 distance and 6.7 torsional restraints per residue, we had a sufficient number of restraints to model a high resolution structure.

Thirty candidate structures were generated from SA using the NMR-derived restraints. Two criteria were used to evaluate the 30 models: the energy of the model (sum of van der Waals and coulomb forces); and the number of distance and torsion angle violations. When the structures had been minimized after SA, the energies ranged from 117 to 477 kcal/mol. A grouping of nine low energy structures was discerned from an examination of the energy distribution. Since crosspeak measurements are not always reliable, the most common high energy distance and torsional violations were eliminated from the restraint set. The most frequent violations were NOEs between H2'/H6 and H3'/H6 of acp^{3}U and the torsion angles between 5''/P, 5'/P and 5'/4' on acp^{3}U.

An important key to structural refinement was localization of the metal binding site. The effect of Mg^{2+} on the CD spectra was small but consistent with the presence of acp^{3}U in the oligomers. Mn^{2+}, which can substitute for Mg^{2+} in biological systems,[9,10] has been used as a paramagnetic probe to determine Mg^{2+} binding sites in biomolecules.[11,12] Mn^{2+} induced the same changes in the CD spectrum of D-acp^{3}U-A as did Mg^{2+} (data not shown). To determine the metal binding site, Mn^{2+} was added to the sample at ion to trimer ratios of 0.008 and 0.05, and ^{1}H and ^{31}P NMR spectra were collected at each step. Only one set of broadened ^{1}H signals were observed indicating that the binding of Mn^{2+} to D-acp^{3}U-A was in fast exchange on the NMR time scale. Manganese broadened the peaks assigned to the α-acp^{3}U, ß-acp^{3}U, γ-acp^{3}U, and 5''-acp^{3}U protons more than other signals in the

Table II. Distances (Å) for the D-acp^{3}U-A Compound with Mg^{2+} Calculated Using SA and Restrained Molecular Mechanics

	Intranucleotide Ribose-Ribose				Base-Base			Ribose-Base		
NOE	D	acp^{3}U	A	NOE	D	acp^{3}U	NOE	D	acp^{3}U	A
1'/2'	2.6-3.9	2.2-3.2	2.2-3.2	5/6	2.0-2.9	1.9-2.8	1'/6or8	2.7-3.9	2.2-3.3(0.2)	2.4-3.6(0.2)
1'/3'	2.5-3.7	2.4-3.6(0.1)	2.5-3.6(0.2)	α/ß1		2.1-3.1	2'/6or8	1.9-2.9		2.1-3.1(0.2)
1'/4'	2.3-3.3(0.3)	2.1-3.1(0.2)	2.4-3.5	α/ß2		2.2-3.2	3'/6or8	2.7-3.9		2.3-3.3
2'/5'	2.3-3.4(0.7)			γ/ß1		2.1-3.1	4'/6or8	3.1-4.5	2.1-3.1(0.8)	2.6-2.9(0.3)
3'/5'		2.8-4.2		γ/ß2		2.3-3.3	5'/6		3.2-4.7	
3'/5'		3.2-4.8					5''/6		2.8-4.2	
4'/5'	2.1-3.1									
4'/5'	2.1-3.1	2.0-2.9								

Internucleotide distances (Å)

NOE	distance	NOE	distance	NOE	distance
H2'(acp^{3}U)-H8(A)	3.0-4.5	H3'(acp^{3}U)-H4'(D)	2.5-3.6 (0.2)	Hß1(acp^{3}U)-H5(D)	2.4-3.5
H3'(acp^{3}U)-H8(A)	2.7-4.0	H6(acp^{3}U)-H3'(D)	3.1-4.5 (0.1)	Hß2(acp^{3}U)-H5(D)	2.46-3.6
Hγ(acp^{3}U)-H3'(A)	2.4-3.5	H6(acp^{3}U)-H4'(D)	3.2-4.7	Hα(acp^{3}U)-H6(D)	2.6-3.8 (0.3)
				Hγ(acp^{3}U)-H4'(D)	1.9-2.9 (0.1)

Violations > 0.1Å are shown in parentheses to the right. An underscore indicates a violation to the lower bound.

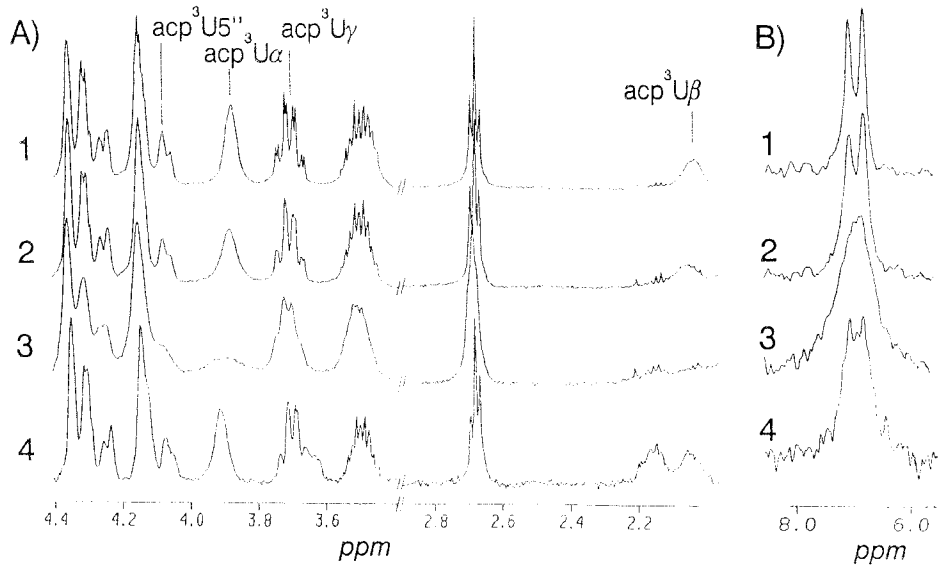

FIG 6: One-dimensional proton (A) and ^{31}P spectra (B) of the D-acp^{3}U-A molecule in D_2O without phosphate buffer at 10°C. Traces 1–3 contain 0, 0.012 and 0.075 mM Mn^{2+}, respectively. Trace 4 is a back titration with 15 mM Mg^{2+}. In the absence of phosphate buffer, the two β-acp^{3}U protons are equivalent (Figure 6, trace 1); however, non-equivalence is returned with the addition of 15 mM Mg^{2+} (Figure 6, trace 4) or phosphate buffer (Figures 4; 2.0–2.2 ppm). The non-equivalences of the protons has been attributed to a possible hydrogen bonding of the side chain to one of the two carbonyls.[18]

spectrum (Figure 6A traces 1-3). The broadness of the first three ^1H signals was consistent with the effect of Mg^{2+} on the signals of the acp^3 side chain.

The H5'' of acp^{3}U is too distant from the side chain of acp^{3}U to be broadened by the same Mn^{2+} that affected the side chain. A second metal ion binding site near the phosphate backbone could explain the paramagnetic broadening of the H5'' of acp^{3}U. The observed selective major broadening of one of the ^{31}P signals confirmed a second potential metal ion binding site assigned to the 5' phosphate of acp^{3}U (Figure 6B traces 1-3). The sample was back-titrated with Mg^{2+} to a maximum of 15 mM in order to demonstrate the reversibility of the Mn-induced broadening (Figures 6A and 6B, trace 4).

The final phase of modeling was construction of the Mg-bound D-acp^{3}U-A structure with Mg^{2+} preferentially interacting with the charged acp^3 side chain. Two local energy minima were discovered for Mg^{2+} in the vicinity of the acp^3 side chain.

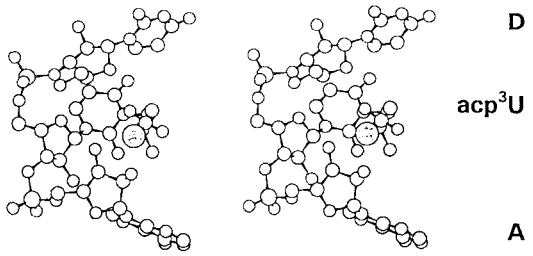

FIG 7: Energy minimized stereoscopic view of D-acp^{3}U-A with Mg^{2+} bound. Mg^{2+} is shown (shaded) with an ionic radius of 0.65Å.

One had Mg^{2+} located 2.18 Å from the δ carbon of acp^{3}U in the O-C-O plane. The other minimum had Mg^{2+} coordinated between one carboxyl oxygen of acp^{3}U and the O2' and O3' of adenosine. When the model was minimized with Mg^{2+} in the O-δC-O plane, the acp^3 side chain extended away from the bases and the trimer lost its coherent shape eliminating this location as a possible solution. However with Mg^{2+} between acp^{3}U and A, the structure was stable. Neither CD nor NMR studies of D-acp^{3}U-A with Mg^{2+} detected a conformational change in adenosine, although adenosine did seem necessary for Mg^{2+} binding based on CD data. CD and NMR distance constraints were satisfied in the structure wherein Mg^{2+} coordinated between acp^{3}U and A.

Paramagnetic NMR experiments with Mn^{2+} suggested that a second Mg^{2+} ion may be binding to the backbone. The number and position of sodium ions had little effect on backbone conformation. However, energy minimization with one Mg^{2+} placed at the backbone yielded an atomic rms difference of 0.92 Å from the configuration using two sodium atoms instead. This difference was mainly due to the χ angle of adenine changing from 166° with Mg^{2+} and Na^+ to -155° with Na^+ alone. The difference becomes smaller (0.21 Å) when only the backbone is considered. Therefore, for the final model to be electrically neutral, we chose to place a single Mg^{2+} between acp^{3}U and adenosine and a single Na^+ by the acp^{3}U phosphorous (Figure 7). An rms difference of 1.10 Å was found when this model was minimized with and without applying distance restraints; the backbone rms difference was 0.19 Å. Table III lists the conformational parameters of the model.

Table III. Torsion Angles[a] of the Energy-Minimized D-acp^{3}U-A Structure

Residue	ß	γ	ϵ	χ	P
D(1)	--	70	113	-121	2'-endo
acp^{3}U(2)	-48	-160	-169	158	2'-exo
A(3)	-166	69	--	-144	3'-endo

[a]Angles are defined as O5' - ß - C5'- γ - C4' - C3' - ϵ - O3'

Discussion

Modified nucleosides contribute unique local conformations to RNA structure.[1] Saturation of the C_5-C_6 bond of D induces a significant conformational change in its sugar pucker to 2'-endo. When uracil in the first position of UUA was replaced with D, DUA, the ribose conformation of the adjacent uridine and adenosine became 72% and 65% 2'-endo, respectively. Residues located 3' to D in the D loop of tRNA crystals also favor the 2'-endo conformation.[8] In the crystal structure of tRNA^{Phe}, the D loop has a high occurrence of 2'-endo sugar pucker located 3' from the two D nucleotides.[6] In contrast, nucleosides 5' adjacent to D retain the common 3'-endo conformation. Thus, D is responsible for the 2'-endo conformation of nucleosides in the 3' direction from its position in tRNAs. Since no known protein or nucleic acid interaction has been directly attributed to the D residue, it is reasonable to assume that its function might have a more subtle structural role. Disruption of base stacking due to elimination of π-π interactions and 2'-endo conformation may be factors that stabilize the tertiary base pairs formed between conserved residues in the D and T loops of tRNAs. In the 2'-endo conformation the phosphate-phosphate distances of the RNA backbone are extended by an additional angstrom over a 3'-endo conformation. In this more extended conformation the bases can present more ligands for interaction with metals or proteins.

The sugar of the mononucleoside of acp^{3}U is 40% 2'-endo. An increased fractional population of the 2'-endo conformer is conferred by the presence of adjacent nucleotides. In the trimers, acp^{3}U is 65% 2'-endo whether D or U is 5'-adjacent; in the dimer, D-acp^{3}U, the conformation is 47% 2'-endo. An interaction of

the acp^3 side chain with the 3'-adjacent nucleotide, in particular, drives the sugar pucker in the direction of 2'-endo. The acp^3 modification is also responsible for the chelation of Mg^{2+}. Thus, the side chain has contributed both chemistry and structure to the oligonucleotides. The modified mononucleoside acp^{3}U does not exhibit a detectable major conformational change in the presence of Mg^{2+}. However, all of the components for metal binding are contained in the small trinucleotide, D-acp^{3}U-A. The 3' adjacent A was required in the trimers to provide suitable ligands for metal coordination. D improved metal binding over U at the first position of the trimer, possibly through its effect on sugar pucker. In the presence of Mg^{2+}, the already large 2'-endo fractional populations of D and acp^{3}U were increased even further in the trimer; D approached nearly 100% 2'-endo and acp^{3}U became 68% 2'-endo. Nucleic acids require counterions to neutralize the large negative charge density. The extra negative potential introduced by acp^{3}U can be effectively balanced with a divalent Mg^{2+} ion.[13]

In the absence of information about Mg^{2+}, modeling of D-acp^{3}U-A predicted a Mg^{2+} binding site of low potential energy. With careful selection of partial charges of acp^{3}U, the model could be used to determine the point of Mg^{2+} binding and which ligands were involved. NMR spectra collected in the presence of Mn^{2+} confirmed Mg^{2+} coordination to the side chain. Only one well defined NOE restraint, D4' to acp^{3}U3', was essential to retain the structure obtained by applying all NMR restraints to the model. Just two conflicts exist between the model and the NMR data; acp^{3}U exhibited β^- and γ^t conformations in the model instead of the standard β^t and γ^+ determined from the coupling constants. Improved parameterization of the modified nucleosides with *ab initio* methods would eliminate such violations.

None of the five tRNA^{Asn} and two tRNA^{Val} molecules known to contain the D-acp^{3}U-A sequence[5] have been analyzed by x-ray crystallography. D(A,C,G)-acp^{3}U-A sequences are known to occur at positions 19-21 in 20 tRNAs for asn and val, arg, leu and tyr, respectively. Eukaryotes favor acp^{3}U at position 20 whereas procaryotes place the same modification at position 47.[5] The adenine at position 21 of D_{19}-acp$^3U_{20}$-A_{21} is an invariant nucleoside of tRNA sequences and is stacked between purine$_{46}$ and pyrimidine$_{48}$ of the variable loop in tRNA crystal structures. With one exception, tRNAs with acp$^3U_{20}$ have the sequence m^7G_{46}-D_{47}-C_{48} in the variable loop.

Nineteen tRNAs for phe, met, arg and tyr that have acp^3U in the sequence m^7G_{46}-acp^3U_{47}-C_{48} in the variable loop, have the sequence $G_{19}D_{20}A_{21}$ in the D loop. Thus, complementary chemistries and conformations must occur between acp^3U_{20} and D_{47}, and D_{20} and acp^3U_{47} in the two trinucleotide sequences brought together in the tertiary structures of these 39 tRNAs.

The global stability added to tRNA by modifications and Mg^{2+} binding has been recognized as an important factor in function.[1] Changes in local charge density, formation of fine structures and increased dynamics in loop regions are important factors in RNA/RNA and protein/RNA interactions. D and acp^3U are examples of how specific modified nucleosides add new chemistries to RNA. D offers a method of introducing 2'-endo interruptions in A-RNA structures, whereas acp^3U offers a method of introducing Mg^{2+} into an RNA for use as a potential catalytic site. Glycine adducts of uracil, similar to acp^3U, have been produced under prebiotic conditions[14] and could have been catalytic molecules in the RNA World. Mg^{2+} continues to be important as a catalytic metal in ribozymes.[15]

Experimental

Sample preparation. The synthesis,[16,17] purification and characterization of the nucleosides D and acp^3U and the oligomers D-acp^3U, UUA, U-acp^3U-A, DUA, and D-acp^3U-A (Figure 1) were described previously.[18] Solution conditions for CD studies were: 10 mM sodium phosphate buffer, pH 7.0, and a sample concentration of 70 nM.[19,20,21] Sample concentrations were determined by UV measurements at 260 nm using a molar extinction coefficient of 5,800 cm^{-1} M^{-1} for oligonucleotides containing D and 8,700 cm^{-1} M^{-1} for the other oligonucleotides.

NMR samples of D-acp^3U-A were prepared by dissolving lyophilized trimer in 98% D_2O containing 10 mM sodium phosphate, pH 7.0. The concentration was estimated to be 8 mM. Two samples, at a concentration of 1.5 mM, were used for the paramagnetic substitution with manganese. One sample was prepared in 10 mM sodium phosphate, pH 7.0, 98% D_2O and the other was in 98% D_2O.

Circular dichroism spectroscopy and Mg^{2+} titrations. In order to maintain a constant sample concentration, D, acp^3U, D-acp^3U, U-U-A, U-acp^3U-A, D-U-A and D-acp^3U-A were titrated with magnesium by dissolution of lyophilized aliquots of

$MgCl_2$ with solutions of the nucleosides.[20] For each sample, CD spectra were gathered at concentrations of 0, 1, 2, 3, 5, 10 and 20 mM Mg^{2+} over a spectral range of 200 to 350 nm. Spectra were recorded using a Jasco J600 spectropolarimeter interfaced to an IBM PS/2 microcomputer.[21] Temperature of the titrations was maintained at 10°C by circulating water through a jacketed cylindrical sample cell. Depending on concentration, cuvettes with cell paths of 1 or 10 mm were used to maintain optimum optical conditions. All CD data were baseline corrected to eliminate contributions from the buffer.

NMR data analysis and spectroscopy. Scalar ^{1}H-^{1}H, ^{1}H-^{31}P, and ^{13}C-^{31}P coupling constants were determined from collected spectra and spectral simulations.[18] Signal assignments of the mononucleosides and various oligomers have been reported.[8,22] In most cases, preliminary values for ^{1}H-^{1}H coupling constants in the ribose ring could be determined from the multiplet splittings of the one-dimensional spectrum. ^{1}H-^{31}P coupling constants were estimated using the results from broadband phosphorous decoupling and from previous experience with modified uridine dimers.[22] The difference in hertz between the outer components of a multiplet represents the sum of its coupling interactions, as long as the multiplet is sufficiently removed from its coupling partners. The difference between ΣJ for the 3' and 5' protons (ΣJ = ΣJcoup - ΣJdec) yields an estimate of the phosphorous coupling that was used to initiate spectral simulations with the PMR program (Serena Software). Conformational parameters were determined using the following relationships: the proportion of 3'-endo conformer $\%N = [(7.5 - J_{1'2'})/6] \times 100$; $\%\gamma^+ = 6[(13.75 - J_{4'5'} - J_{4'5''})/10.05] \times 100$[23]; $\%\epsilon^t = [(J_{C4'P3'} - 0.4)/7.1] \times 100$. $\%\beta^t(^1H) = [(25.5 - J_{5'P} - J_{5''P})/20.5] \times 100$. Classification of the glycosidic angle, χ, was based on the relative magnitude of NOE connectivities of H6/H2' > H6/H1' = anti, and H6/H1' > H6/H2' = syn.

ROESY spectra of D-acp^{3}U-A were acquired at 15°C with 512 blocks and 1024 data points per block and with mixing times of 100, 300 and 600 ms. Felix 2.0 (Biosym Technologies) was used to process the data using a 15° phase shifted sine bell function and then zero-filled to 1K x 1K matrices. ROESY crosspeaks from the 100 and 300 ms mixing times were used to determine proton distances.

The influence of Mg^{2+} on the conformation of D-acp^{3}U-A was monitored by observing spectral variations in the ^{1}H, ^{13}C and ^{1}H-decoupled ^{31}P NMR spectra during

a seven step titration from 0 to 20 mM Mg^{2+} at 10°C. Further localization of the metal ligands was determined by monitoring peak widths during Mn^{2+} titration and a Mg^{2+} back-titration. Two Mn^{2+} titrations were performed, one in the presence of phosphate buffer and the other in its absence. Without the competition from the phosphate buffer for Mn^{2+} ions in solution, less Mn^{2+} was needed to induce the same NMR line-broadening though the final results were the same. ^{31}P spectra were referenced to trimethyl phosphate and ^{1}H spectra were referenced to DSS.

Structural Modeling. Three-dimensional structures of the D-acp^{3}U-A were constructed and modeled using Insight II/Discover 2.2 (Biosym Technologies) on an Indigo Silicon Graphics workstation. Structure determination was accomplished in three phases: i) generation of a set of candidate structures using simulated annealing (SA) with NMR restraints starting from random coordinates; ii) further refinement by dynamics of selected low energy structures using relaxed restraints; and iii) extensive structure refinement using reparameterized nucleotides and metal ions. Distance restraints were obtained from NOEs by scaling the measured peak volumes to the H5/H6 NOEs of acp^{3}U (distance 2.45 Å) of the 100 and 300 ms ROESY spectra. No additional interresidue scalars were used since no other fixed distances in D-acp^{3}U-A were known. Angle restraints from $^{3}J_{HH}$ coupling constants were calculated from COSY spectra using the Karplus relation with the constants from Davies.[24] The forcing potential for the distance and dihedral restraints took the form:

$$F_{dc} = 0 \begin{cases} k_u(r_{ij} - r_{ij}^{u})^2 & r_{ij} \geq r_{ij}^{u} \\ r_{ij}^{l} < r_{ij} < r_{ij}^{u} & \\ k_l(r_{ij} - r_{ij}^{l})^2 & r_{ij} \leq r_{ij}^{l} \end{cases} \quad (1)$$

where r_{ij}^{u} and r_{ij}^{l} are the upper and lower bounds of the target distance and angular restraints, k_u and k_l the force constant (k_{dist}=10 kcal·mol^{-1}·Å^{-2}, $k_{diheral}$=1 kcal·mol^{-1}·rad^{-2}) and r_{ij} the measurement between atoms i and j in the model. Distance restraints had upper and lower bounds of 15% and corrections for pseudoatom representation were applied to non-stereo-specifically assigned protons.[25] Upper and lower bounds of 10° were placed on the Karplus solutions.

SA was initiated with random atomic coordinates and the consistent-valence force field[26] with automatically assigned parameters and no charges. The following stages

were used for the SA protocol: i) Each structure was minimized with 100 steps of steepest decent followed by 500 steps of conjunctive gradient until the maximum derivative was <0.01 kcals/Å; ii) Molecular dynamics was performed for 30-ps at 1000°K while scaling the restraints, derived from ROESY spectra and coupling constants, from 0.1% to their full value; iii) Ten-ps of dynamics at 1000°K, scaling the covalent terms to their full values; iv) Before allowing the system to cool, the distance and torsional restraints were scaled to twice their value, 20 kcal·mol^{-1}·Å^{-2} and 2 kcal·mol^{-1}·rad^{-2}, respectively, and the non-bond interactions were scaled from 15 to 25% of their value; v) The system was cooled to 300°K following a geometric progression over 10-ps; vi) The system was minimized using the same routine as in the first stage. For the nine lowest energy structures an additional 30 ps of molecular dynamics were run. During the dynamics simulation, the restraints were relaxed to 5% during the first 15 ps of the simulation and restored to 100% during the remaining 15 ps. This was followed by 600 steps of energy minimization.

The final refinement involved extensive energy minimization using the AMBER force field[27] with the single lowest energy model from the previous phase that best fit the known conformational parameters. Additional parameterization of D and acp^{3}U, using the MNDO[28] Hamiltonian and the electrostatic potential method in MOPAC6,[29] was required to better represent these nucleosides in the AMBER force field. Electrostatic potentials calculated for D and acp^{3}U were compared with the AMBER partial charges of uridine and uridylic acid, respectively. For acp^{3}U partial charges of the acp side chain were scaled and then adjusted to create a -1 charge group that could be integrated with the AMBER parameters. All restrained energy minimizations began with the lowest energy model from the dynamic calculations. Unless otherwise noted, energy minimizations used 100 steps of steepest decent followed by 500 or more steps using the quasi-Newton-Raphson algorithm[30] until the maximum derivative was ≥ 0.001 kcal/Å. Additional computational parameters were: no nonbonded cutoff was set; an implemented distance dependent dielectric ($\epsilon = 4r_{ij}$/Å); the 1-4 nonbond interactions were scaled by a factor of 0.5.

Acknowledgements

Support was provided by the National Institutes of Health Grant GM23037-14 (PFA) and the Polish Committee for Scientific Research PB0506/P3/93/05 (AM).

Supplemental Table. ^1H-^1H Coupling Constants[a] and Changes Produced by Addition of Mg^{2+} [b]

	D	acp^{3}U	D------acp^{3}U		D------acp^{3}U------A			D---------U---------A			U------acp^{3}U-------A			U---------U---------A		
1'2'	6.8	3.9	7.2	4.3	7.3	5.3	5.3	7.2	5.8	5.4	4.9	5.4	5.2	4.6	4.3	4.2
					+0.3	*+0.3*										
2'3'	5.8	5.5	5.4	5.5	5.3	6.0	5.3	5.4	5.0	5.4	5.1	6.1	5.2	5.2	4.9	5.1
3'4'	3.8	5.8	2.7	4.8	--	3.9	5.4	4.0	5.2	5.5	5.1	4.0	5.4	5.2	5.0	5.3
3'P	--	--	8.1	--	8.4	9.6	--	8.3	8.4	--	8.3	9.6	--	8.0	8.4	--
4'5'	3.2	2.7	3.2	2.3	3.4	1.4	2.4	3.3	2.9	2.5	2.8	1.8	2.6	2.6	2.8	2.3
4'5''	5.1	4.4	4.6	3.1	4.5	3.1	3.4	4.5	3.9	3.6	3.2	3.2	3.4	3.8	3.9	3.3
5'5''	12.5	12.8	12.6	11.3	12.7	11.6	12.0	12.5	13.0	12.0	12.5	12.0	12.0	12.9	12.9	12.0
					-0.3	*+0.2*										
5'P	--	--	--	4.6	--	4.6	4.3	--	4.2	4.4	4.8	4.6	4.3	5.0	4.0	4.2
5''P	--	--	--	4.6	--	3.8	4.1	--	--	4.3	--	3.8	4.2	--	--	4.1
5,6	6.4	7.9	6.4	7.9	6.6	8.0	--	6.5	8.1	--	8.1	7.8	--	8.1	8.1	--
					+0.2											
acp^{3}U α,β	--	6.9	--	7.5	--	7.9	--	--	--	--	--	7.8	--	--	--	--
acp^{3}U β,γ	--	7.4	--	5.1	--	5.3	--	--	--	--	--	5.2	--	--	--	--
NOE[c]	2' > 1'	2' ~ 1'	2' ≫ 1'	2' > 1'	2'	2' > 1'	2' ≫ 1'	2' > 1'	2' > 1'	2' ≫ 1'	2' > 1'	2' > 1'	2' > 1'	2' ~ 1'	2' ~ 1'	2' ~ 1'

[a]In deuterated PBS; absolute value in hertz.
[b]Changes, whether negative or positive, observed with the addition of Mg^{2+} to D-acp^{3}U-A are denoted in *italics* under the coupling constant.
[c]NOE observed from H6 or H8.

REFERENCES

1. Agris, P. F. *Prog. Nucl. Acids Res. Mol. Biol.* in press.
2. Limbach, P. A.; Crain, P. F.; McCloskey, J. A. *Nucl. Acids Res.* **1994**, *22*, 2183-2196.
3. Emerson, J.; Sundaralingam, M. *Acta Cryst.* **1980**, B*36*, 537-543.
4. Cadet, J.; Ducolumb, R.; Hruska, F. E. *Biochim. Biophys. Acta* **1980**, *563*, 206.
5. Steinberg, S.; Misch, A.; Sprinzl, M. *Nucl. Acids Res.* **1993**, *21*, 3011-3015.
6. Westhof, E.; Dumas, P.; Moras, D. *Acta Cryst.* **1988**, A*44*, 112-123.
7. Nawrot, B.; Malkiewicz, A. *Nucleosides & Nucleotides* **1992**, *11*, 1455-1461.
8. Smith, W. S.; Nawrot, B.; Malkiewicz, A.; Agris, P. F. *Nucleosides & Nucleotides* **1992**, *11*, 1685-1694.
9. Craik, D. H.; Higgins, K. A. *Annu. Rep. Nucl. Magn. Reson. Spectr.* **1989**, *22*, 61-138.
10. Hurd, R. E.; Azhderian, E.; Reid B. R. *Biochemistry*, **1979**, *18*, 4012-4017.
11. Ott, G.; Arnold, L.; Limmer, S. *Nucl. Acids Res.* **1993**, *21*, 5859-5864.
12. Chao, Y.; Kearns, D. *Biochem. Biophys. Acta* **1979**, *477*, 20-27.
13. Honig, B.; Nicholls, A. *Science* **1995**, *268*, 1144-1149.
14. Robertson, M. P.; Miller, S. L. *Science* **1995**, *268*, 703-705.
15. Pyle, A. *Science* **1993**, *261*, 709-714.
16. Ohtsuka, E.; Ikehara, M.; Soll, D. *Nucl. Acids Res.* **1982**, *10*, 6553-6570.
17. Reese, C. B. *Tetrahedron* **1978**, *34*, 3143-3179.
18. Nawrot, B.; Malkiewicz, A.; Smith, W.; Agris, P. *Nucleosides & Nucleotides* **1995**, *14*, 143-165.

19. Guenther, R. H.; Hardin, C. C.; Sierzputowska-Gracz H.; Agris, P. F. *Biochemistry* **1992**, *31*, 11004-11011.

20. Dao, V.; Guenther, R. H.; Agris, P. F. *Biochemistry* **1992**, *31*, 11012-11019.

21. Chen, Y.; Sierzputowska-Gracz, H.; Guenther, R. H.; Everett, K.; Agris, P. F. *Biochemistry* **1993**, *32*, 10249-10253.

22. Smith, W. S.; Sierzputowska-Gracz, H.; Sochacka, E.; Malkiewicz, A; Agris, P. F. *J. Amer. Chem. Soc.* **1992**, *114*, 7989-7997.

23. Chladek, S.; Kumar, G.; Celewicz, L. *J. Org. Chem.* **1982**, *47*, 634-644.

24. Davies, D. B. *Prog. NMR Spec.* **1978**, *12*, 135-225.

25. Wüthrich, K.; Billeter, M.; Braun, W. *J. Mol. Biol.* **1983**, *169*, 949-961.

26. Dauber-Osguthorpe, P.; Roberts, V. A.; Osguthorpe, D. J.; Wolff, J.; Genest M.; Haggler, A. T. *Proteins Struct. Funct. Genet.* **1988**, *4*, 31-47.

27. Weiner, S. J.; Kollman, P. A.; Nguyen, D. T.; Case, D. A. *J. Comp. Chem.* **1986**, *7*, 230-252.

28. Dewar, M. J. S.; Bingham, R. C.; Lo, D. H. *J. Am. Chem. Soc.* **1977**, *99*, 4899.

29. Besler, B. H.; Merz, K. M.; Kollman, P. A. *J. Comp. Chem.* **1990**, *11*, 431-439.

30. Fletcher, R. *Practical Methods of Optimization*, Volume 1; John Wiley & Sons: New York, 1980.

Received August 24, 1995
Accepted December 18, 1995